Beam–Cavity Interaction Circuit at W-Band

Marc E. Hill, W. R. Fowkes, X. E. Lin, and David H. Whittum

***Abstract*—In this paper, we describe the design, fabrication, and bench study of a millimeter-wave cavity employed as a relativistic klystron output structure. The oxygen-free electronic-grade copper cavity was prepared by electro-discharge machining and diffusion bonding, and cleaned and tuned to 91.4 GHz. Measured cavity characteristics are presented and compared with theory, including quality factor Q, coupling parameter β, scattering matrix S_{11}, and axial electric field profile E_z. This paper provides the basis for an understanding of the cavity as a transfer structure.**

I. Introduction

High-energy physics requires compact accelerators operating at extreme gradients, in excess of 100 MV/m. Scalings for trapping, pulsed heating, and other high-gradient phenomena favor miniature short-wavelength structures to hold off the large electric fields required [1]. A critical problem in the practical study of such a structures is the absence of a high-power millimeter-wave source. Study of high-field phenomena at conventional wavelengths has required the development of high-power klystrons over several decades of research and engineering [2]. For millimeter-wave accelerators, we are approaching the corresponding learning curve for high-power handling by a different route, employing an existing accelerator to power millimeter-wave transfer structures, much as in a relativistic klystron. The benefit of such work is the development of know-how in miniature structure fabrication, bench-test, and high-field studies in an accelerator beam environment, in parallel with millimeter-wave klystron development [3].

Here, we report theory and measurements for a single miniature cavity with WR10 output, and 680-μm-diameter beam tube, prepared for excitation by a relativistic electron beam. This paper establishes that the 3.3-mm wavelength (91.4 GHz) scale is accessible to modern machining and measurement techniques, and provides the basis for the understanding of cavity performance as a transfer structure.

II. Tolerances

To appreciate the machining and tuning tolerances involved, it is helpful to consult the circuit-equivalent picture of the application, as seen in Fig. 1. A beam bunched at 11.424 GHz passes through the beam tube, exciting the cavity resonance at the eighth beam harmonic, i.e., 91.392 GHz. The beam pulse length of 100 ns is much longer than the loaded fill time of the cavity ($T_f \approx 1.5$ ns) so that steady state is reached early in the pulse. In steady state, the cavity voltage $\tilde{V}_c$ may be expressed in terms of the beam current $\tilde{I}_b$ as [4]

$$\tilde{V}_c = -\frac{1}{2}\cos\psi e^{j\psi} Q_L \left[\frac{R}{Q}\right] \tilde{I}_b \tag{1}$$

where the beam-coupling parameter "R-over$Q$" is defined according to

$$\left[\frac{R}{Q}\right] = \frac{|\tilde{V}_c|^2}{\omega_0 U} \tag{2}$$

Manuscript received July 25, 1999. This work was supported by the U.S. Department of Education under Contract DE-AC03-76SF00515.

M. E. Hill is with the Physics Department, Harvard University, Cambridge, MA 02138 USA.

W. R. Fowkes, X. E. Lin, and D. H. Whittum are with the Stanford Linear Accelerator Center, Stanford University, Stanford, CA 94309 USA.

Publisher Item Identifier S 0018-9480(01)03324-5.

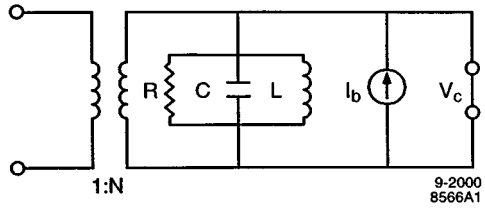

Fig. 1. Circuit equivalent for beam interaction with a single cavity with waveguide output. In the relativistic limit, beam-loading admittance is negligible.

in terms of stored energy U and resonance angular frequency ω_0. The tuning angle ψ is defined in terms of the loaded quality factor Q_L and the drive angular frequency ω according to

$$\tan\psi = Q_L\left(\frac{\omega_0}{\omega} - \frac{\omega}{\omega_0}\right). \tag{3}$$

Power radiated by the cavity into the guide may then be determined according to

$$P_{out} = \frac{|\tilde{V}_c|^2}{Q_e\,[R/Q]} \tag{4}$$

where Q_e is the external quality factor. From this, one may show that a 10% reduction in power corresponds to a tuning angle of $\tan\psi = 1/3$ or cell detuning of $\delta\omega/\omega \approx 1/6Q_L$. For a loaded quality factor, $Q_L \approx 415$.

III. Fabrication and Assembly

The completed geometry is indicated in Fig. 2. Next, we describe how this geometry was accomplished, with a set of four nominally identical cavities.

The oxygen-free electronic grade (OFE) copper cavity consists of three layers: a 2.44-mm-thick plate with the cavity wire electro-discharge machined (EDM) and two featureless plates comprising the cavity top and bottom. (The orientation of the cavity "top" is at positive x in Fig. 2 and the "bottom" is at negative x.) The three layers were diffusion bonded together employing a 1024 °C heat cycle at 25 lbs/in^2 for 10 min. The input waveguide coupling iris was then cut using sinker EDM. Ultrasonic acetone rinse had no measurable effect on the wall quality factor, and the cavity was subjected to chemical cleaning. This raised the wall Q (prior to cutting of the beam tube) from 1029 to 1252.

A threaded bolt circle conforming to a WR10 0.75-in flange was machined into the waveguide opening for each cavity. The width ("a" dimension) of the waveguide openings were intended to match the 0.1-in-wide dimension of WR10 guide, but were accidentally machined 0.1 mm narrower, resulting in a step on each side of the connecting waveguide. Analysis indicated that this would have negligible effect on the measurements.

To cut the beam tubes, we used a sinker EDM for the first rough cut of the cavity. We then made a final cut of the 340-μm radius using a wire EDM. To remove any debris created by the EDM process on the surfaces of the cavity walls, we etched the cavity by pumping an acid solution through the coupling port of the cavity.

IV. Measurements

To determine the state of the cavity, and as an aid in tuning, we employed a home-built W-band vector network analyzer (VNA). The

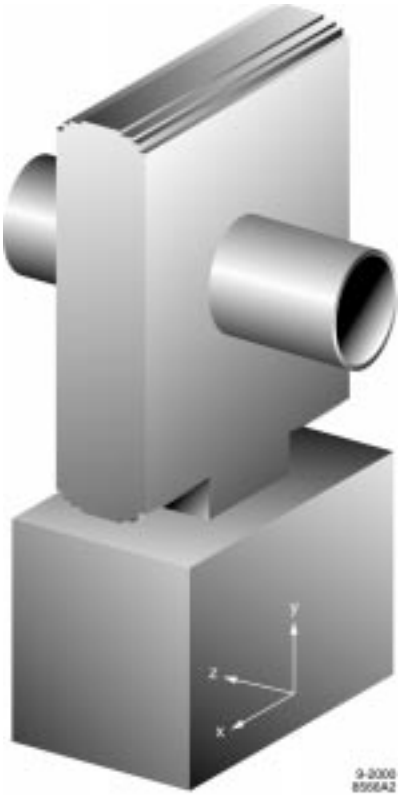

Fig. 2. Geometry of the interior conducting boundaries of the cavity, including coupling iris, beam-tube, and WR10 output. The mesh shown is that employed for numerical simulations.

VNA permits measurement of the steady-state complex reflection coefficient $\tilde{S}_{11}$ over a range of angular frequencies ω. This may be compared with the theoretical result for single-mode excitation of a resonator [4]

$$\tilde{S}_{11} = \frac{2\beta}{1+\beta}\cos\psi e^{j\psi} - 1. \tag{5}$$

The coupling parameter $\beta = Q_{\rm w}/Q_{\rm e}$ is the ratio of the wall quality factor to the external (or "diffractive") quality factor. Combining (5) with Slater's theorem, we may infer the electric-field profile by means of a bead pull. In this way, we can have assessed the tune, and $Q_{\rm e}$, $Q_{\rm w}$, and β, as listed in Table I. The measured external quality factor was insensitive to the cleaning steps.

Also seen in Table I are the analytic results for a closed pillbox, and the numerical results for the cavity with beam ports obtained from the finite-difference code *GdfidL* [5]. For analytic comparison, we employed a rectangular pillbox of interior transverse dimensions $a \times b \approx 2.30$ mm $\times$ 2.44 mm and transit length $L \approx 0.50$ mm. The corresponding resonance angular frequency is given by $\omega_0 = \beta_0 c$, where

$$\beta_0 = \sqrt{\frac{\pi^2}{a^2} + \frac{\pi^2}{b^2}} \tag{6}$$

with $c \approx 2.9979 \times 10^8$ m/s the speed of light. This gives a frequency of 89.6 GHz; accounting for the volume change due to the fillets from an 8-mil-diameter EDM wire (about 0.8%), we calculate the resonance frequency to be 90.1 GHz. The measured frequency of the four cavities varied between 90.1–90.8 GHz, variation attributable to wire machining errors. The theoretical wall quality factor for the closed rectangular pillbox geometry may be expressed as

$$\frac{1}{Q_{\rm w}} = 2\frac{R_s}{Z_0}\frac{1}{\beta_0 L}\left\{1 + \frac{2\pi^2 L}{\beta_0^2}\left(\frac{1}{a^3} + \frac{1}{b^3}\right)\right\} \tag{7}$$

with $Z_0 \approx 377\ \Omega$ the impedance of free space, and $R_s \approx 79$ mΩ the theoretical surface resistance of a smooth OFE copper surface at the operating frequency. This corresponds to a wall quality factor of 1.57×10^3.

The external quality factor $Q_{\rm e}$ may be calculated by two methods. One is a simple estimation from power transmission through the coupling iris, obtained from HFSS simulation [6]. With a rectangular iris of width 0.83 mm, height 0.5 mm, and thickness 0.25 mm, we find $Q_{\rm e} = 1400$. A second method utilizes the frequency-domain result of the closed cavity–waveguide system to find the complex resonance frequency of the waveguide loaded cavity [7]. This gives a $Q_{\rm e}$ of 1370 with no beam port. These dimensions correspond to the geometry prior to cutting of the beam tube and the second acid rinse.

The finished assembly, with a beam port, had a wider iris opening of 0.92 mm. For this aperture, the frequency-domain approach gives $Q_{\rm e} \approx 583$, which is lowered due to the resulting stronger external coupling. The sensitivity of $Q_{\rm e}$ to the coupling iris width is noteworthy. A 20-μm-wider iris lowers the $Q_{\rm e}$ by 200, while a 20-μm-thinner iris reduces $Q_{\rm e}$ by 170.

The result for the scattering parameter S_{11} is indicated in Fig. 3, overlaid with the result computed with the time-domain module of *GdfidL*. The simulation employs a damping decrement based on the theoretical wall quality factor $Q_{\rm w} \approx 1540$. The same result is seen in the Smith Chart plot in Fig. 4. There, one can also observe the effect of the chemical cleaning in decreasing the external quality factor. The original iris width was 0.87 mm, and this was widened to 0.92 mm

TABLE I
MEASURED AND THEORETICAL PARAMETERS FOR THE SINGLE-CELL CAVITY WITH AND WITHOUT A BEAM PORT

	No Port	Beam Port
Q_w (analytic)	1574	—
Q_w (simulation)	1533	1540
Q_w (measured)	1252	1305
Q_e (simulation)	1400/1370	583
Q_e (measured)	1048	571
β	1.19	2.29
$[R/Q]$ (simulation)	134 Ω	110 Ω

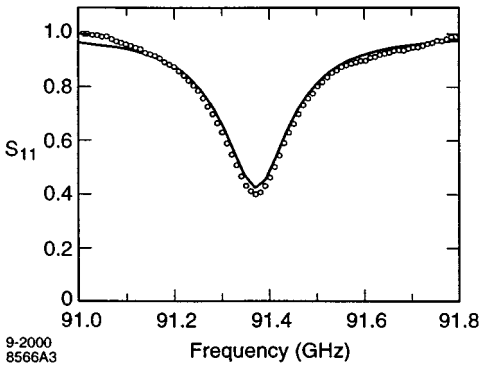

Fig. 3. Reflection coefficient versus frequency (from measurement) and numerical simulation.

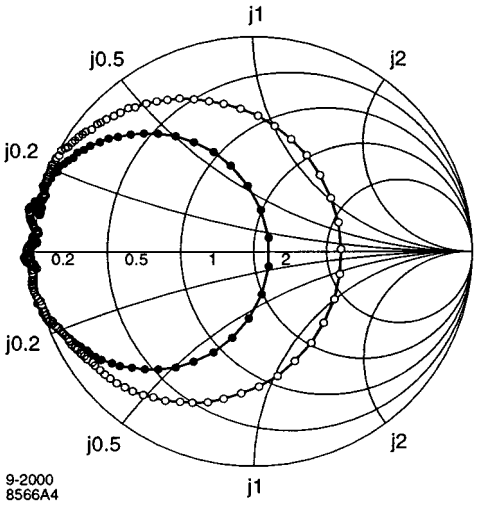

Fig. 4. Smith Chart plot of measured S_{11} for the case of no beam port (black) and with a 680-μm beam port (white). For both cases, we see that the cavity is overcoupled.

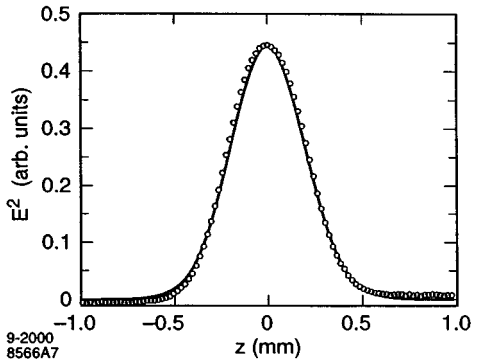

Fig. 5. Result for inferred axial electric field E_z from bead–pull measurement, overlaid with theory. The z-coordinate is as shown in Fig. 2, with the bead pull along the beam axis.

in the course of chemical cleaning. A bead pull was also performed, with the measurement seen in Fig. 5, overlaid with the result computed with the frequency-domain module of *GdfidL*. The dielectric bead was formed by tieing a knot in a length of surgical fiber made of nylon.

The field profile data seen in Fig. 5 permit one to go on to infer peak electric field from cavity voltage, with the result $V_c/E_{\rm pk} \approx 6.14 \times 10^{-4}$ m. Using (4), one may then infer a peak field from the power radiated. With $[R/Q] \approx 110\,\Omega$ from numerical simulation (*GdfidL*), and $Q_e \approx 571$ from measurement, a figure of $P_{\rm out} \approx 1$ kW corresponds to a cavity voltage of 7.9 kV, and a peak field of $E_{\rm pk} \approx 12.9$ MV/m.

V. Conclusions

The bench measurements and simulations presented in this paper indicate that fabrication of and bench measurement on a high-Q millimeter-wave waveguide-coupled resonator are, in practice, quite feasible. Results presented here provide the basis for understanding of the cavity interaction with a beam. This cavity has subsequently been installed on a 300-MeV 0.5-A beam line at the Stanford Linear Accelerator Center (SLAC), Stanford, CA, producing peak power in the range of 1 kW, which will be the subject of a future paper.

Acknowledgment

The authors thank G. Caryotakis, Stanford Linear Accelerator Center (SLAC), Stanford University, Stanford, CA, J. Huth, Harvard University, Cambridge, MA, O. Millican, SLAC, Stanford University, Stanford, CA, D. Shelly, SLAC, Stanford University, Stanford, CA, and A. Farvid, SLAC, Stanford University, Stanford, CA, for their assistance.

References

[1] D. H. Whittum, "Ultimate gradient in solid-state accelerators," in *Proc. Adv. Accelerator Concepts Workshop*.
[2] G. Caryotakis, "High power microwave tubes: In the laboratory and on-line," *IEEE Trans. Plasma Sci.*, vol. 22, pp. 683–691, Oct. 1994.
[3] ——, "The Klystron: A microwave source of surprising range and endurance," *Phys. Plasmas*, vol. 5, pp. 1590–1598, 1998.
[4] D. H. Whittum, "Introduction to Microwave Linacs," in *Techniques and Concepts of High-Energy Physics*, T. Ferbel, Ed. Norwell, MA: Kluwer, 1999, vol. X, pp. 387–486.
[5] W. Bruns, "GdfidL: A finite difference program for arbitrarily small perturbations in rectangular geometries," *IEEE Trans. Magn.*, vol. 32, pp. 1453–1456, May 1996.
[6] *High Frequency Structure Simulator*, Ansoft Corporation, Pittsburgh, PA.
[7] N. M. Kroll and X. E. Lin, "Computer Determinations of the Properties of Waveguide Loaded Cavities," in *Proc. Linear Accelerator Conf.*, C. Beckmann, Ed., Abuquerque, NM, 1990, pp. 238–240.

Design of a Low-Cost 2-D Beam-Steering Antenna Using Ferroelectric Material and the CTS Technology

Magdy F. Iskander, Zhengqing Yun, Zhijun Zhang, R. Jensen, and S. Redd

***Abstract*—The design of a new low-cost antenna array with two-dimensional beam-scanning capability is presented in this paper. The design procedure is based on the continuous transverse stub (CTS) technology and the use of ferroelectric material. With the application of a low-loss ferroelectric material barium strontium titanium oxide with 40% oxide III, beam-scan capability from −60° to 60° was achieved. The tradeoffs in selecting the ferroelectric material and between losses and bias voltage in the CTS design were also examined. Furthermore, it was found necessary to adjust the dimensions of the radiating stubs, as well as the connecting sections of the feed waveguide so as to eliminate reflections between the stubs and, hence, maintain the desirable radiation pattern. It is shown that the use of an average height for the feed waveguide will result in deterioration in the radiation pattern.**

***Index Terms*—CTS, ferroelectric material, low cost, phased array, 2-D beam steering.**

I. Introduction

The design of a low-cost antenna array with two-dimensional (2-D) steering capability is critically important for the commercial success of the satellite industry in broad consumer markets. As the satellite and mobile wireless communications technologies continue to utilize higher frequencies in the 20–60-GHz range, the design

Manuscript received February 1, 2000; revised November 30, 2000.
The authors are with the Electrical Engineering Department, University of Utah, Salt Lake City, UT 84112 USA.
Publisher Item Identifier S 0018-9480(01)03305-1.